Increased lactate/pyruvate ratio augments blood flow in physiologically activated human brain

Mark A. Mintun*, Andrei G. Vlassenko, Melissa M. Rundle, and Marcus E. Raichle

Mallinckrodt Institute of Radiology, Washington University School of Medicine, 510 South Kingshighway Boulevard, St. Louis, MO 63110

Contributed by Marcus E. Raichle, November 10, 2003

The factors regulating cerebral blood flow (CBF) changes in physiological activation remain the subject of great interest and debate. Recent experimental studies suggest that an increase in cytosolic NADH mediates increased blood flow in the working brain. Lactate injection should elevate NADH levels by increasing the lactate/pyruvate ratio, which is in near equilibrium with the NADH/NAD^+ ratio. We studied CBF responses to bolus lactate injection at rest and in visual stimulation by using positron-emission tomography in seven healthy volunteers. Bolus lactate injection augmented the CBF response to visual stimulation by 38–53% in regions of the visual cortex but had no effect on the resting CBF or the whole-brain CBF. These lactate-induced CBF increases correlated with elevations in plasma lactate/pyruvate ratios and in plasma lactate levels but not with plasma pyruvate levels. Our observations support the hypothesis that an increase in the NADH/NAD^+ ratio activates signaling pathways to selectively increase CBF in the physiologically stimulated brain regions.

The nature of the link between cerebral blood flow (CBF) and energy metabolism is of great interest and importance but remains controversial despite decades of research and debate. Although CBF augmentation is still considered to be a hallmark of intensified neural activity, previous assumptions that behaviorally induced increases in local blood flow reflect similar local increases in oxidative metabolism (1) have been contradicted by brain imaging studies with positron-emission tomography (PET) (2, 3) and functional MRI (4). Fox and his colleagues (2, 3) demonstrated that in normal, awake adult humans, stimulation of the visual or somatosensory cortex results in dramatic increases in CBF but minimal increases in oxygen consumption. Increases in glucose utilization are similar to changes in CBF (3, 5). Although it is often assumed that the increase in CBF in neural activation is driven by a need for increased delivery of oxygen or glucose, it has been demonstrated in human subjects that the CBF response to physiological activation is not altered by either stepped hypoglycemia (6) or hypoxia (7). These results suggest that increased CBF during physiological brain activation does not occur to prevent a shortage of these metabolic substrates.

Ido *et al.* (8) recently reported that CBF in activated rat brain is modified by changes in the plasma lactate/pyruvate ratio: CBF was augmented when lactate/pyruvate ratios were raised and attenuated when the ratios were lowered. Specifically, immediately after lactate bolus injection, the magnitude of the CBF increase associated with sensory stimulation approximately doubled. Based on the near equilibrium between the ratios of lactate/pyruvate and cytosolic free NADH/NAD^+ (which reflects the local environment redox state) (9), they suggested that cytosolic free NADH is an important trigger or sensor of blood flow. The reoxidation of NADH to NAD^+ is a step of vital importance for brain cells, especially in the activated state, because without continuing replenishment of NAD^+, glycolysis could not proceed and ATP could not be generated (10). Ido *et al.* (8, 11) have suggested several potential signaling pathways coupled to the reoxidation of NADH to NAD^+ that could mediate physiologically activated CBF. To our knowledge, no data have yet been reported regarding the impact of lactate injection on physiologically activated CBF in humans.

The aim of this study was to evaluate the effect of acute lactate injection on regional CBF at rest and during task-specific functional activity in neurologically normal subjects.

Materials and Methods

Subjects. Seven healthy, right-handed (12) subjects, four females and three males (ages 20–27 years; mean age ± SD was 24.0 ± 2.4 years), were recruited from the Washington University community. The Humans Studies Committee and the Radioactive Drug Research Committee of our institution approved the protocol of this study. Written informed consent was obtained.

PET Imaging. All subjects underwent a single PET session consisting of six CBF scans. Studies were done with a Siemens/CTI ECAT EXACT HR 47 tomograph (Iselin, NJ) (13). This scanner collects 47 simultaneous slices with 3.125-mm spacing encompassing an axial field of view of 15 cm. Transaxial resolution is ≈4.3 mm full-width half-maximum at slice center. Studies were done in the 2D acquisition mode (interslice septa extended). Transmission scans for attenuation correction of all emission data were obtained. All subjects had a radial artery catheter placed under local anesthesia for blood sampling. A 20-gauge i.v. catheter was placed in the antecubital vein and advanced to the axillary vein. This location prevented any local irritation from the lactate infusion.

Each measurement of the CBF was initiated by a bolus i.v. injection of 50 mCi (1 Ci = 37 GBq) of [^{15}O]water and a concomitant 3-min dynamic scan (50 frames: thirty-five 2-sec frames, eight 5-sec frames, and seven 10-sec frames). Arterial blood sampling was done by continuous arterial blood withdrawal over a shielded scintillator to measure blood radioactivity. Twelve minutes were allowed between tracer injections for ^{15}O decay; however, 20 min were allowed after each study with a lactate injection. Measurements of arterial values for pH, carbon dioxide pressure, oxygen pressure, hematocrit, Hb, oxygen saturation, and oxygen content were performed at regular intervals during the study.

Six PET scans were performed on each subject after injection of saline or lactate in the following sequence: scan 1, saline-rest (referred later as CBF_1); scan 2, saline-activation (CBF_2); scan 3, lactate-rest (CBF_3); scan 4, lactate-activation (CBF_4); scan 5, saline-rest (CBF_5); and scan 6, saline-activation (CBF_6). Sixty seconds before scans 1, 2, 5, and 6, the subjects received an injection of 20 ml of saline. Starting 60 sec before scans 3 and 4, the subjects received a rapid i.v. infusion (over 30 sec) of lactate (1 mmol or 90 mg/kg of body weight) diluted in saline to make a total amount of 20 ml. Subjects were blind to the order of saline and lactate.

Arterial glucose, lactate, and pyruvate levels were obtained before and after each PET scan and before and after each lactate injection.

Abbreviations: CBF, cerebral blood flow; PET, positron-emission tomography; VOI, volume of interest.

*To whom correspondence should be addressed. E-mail: mintunm@mir.wustl.edu.

Table 1. Demographic and blood gas data

Subject	Gender	Age, years	pH	$PaCO_2$, mmHg	PaO_2, mmHg	Hematocrit	Hb, g/liter	SaO_2	CaO_2, mL O_2/liter
1	F	20	7.35 ± 0.04	39 ± 2	98 ± 3	0.35 ± 0.01	118 ± 2	0.98 ± 0.00	162 ± 2
2	M	26	7.38 ± 0.00	46 ± 3	87 ± 0	0.37 ± 0.04	121 ± 0	0.99 ± 0.03	166 ± 4
3	F	24	7.42 ± 0.02	33 ± 1	—	0.33 ± 0.00	105 ± 3	0.98 ± 0.00	143 ± 4
4	F	22	7.44 ± 0.04	34 ± 2	100 ± 15	0.26 ± 0.00	84 ± 1	0.98 ± 0.01	114 ± 1
5	F	24	7.48 ± 0.02	34 ± 2	102 ± 9	0.35 ± 0.01	107 ± 1	0.99 ± 0.01	147 ± 1
6	M	25	7.40 ± 0.03	34 ± 1	92 ± 10	0.39 ± 0.01	126 ± 4	0.97 ± 0.01	170 ± 7
7	M	27	7.39 ± 0.02	37 ± 1	109 ± 1	0.45 ± 0.01	166 ± 0	0.99 ± 0.00	221 ± 0

Values are means ± SD. $PaCO_2$, arterial carbon dioxide pressure (1 mmHg = 133 Pa); PaO_2, arterial oxygen pressure; —, not available; SaO_2, arterial oxygen saturation; CaO_2, arterial oxygen content. F, female; M, male.

Visual Stimulation Paradigm. Three PET scans in each subject were done during rest with eyes closed, and three scans were done while each subject looked at a visual stimulus. The visual stimulation paradigm was chosen to produce CBF responses in the moderate range [as opposed to a maximal CBF response, as in Fox *et al.* (2, 3)] to avoid a "ceiling" effect in CBF response. Each subject was presented one of two types of visual grating: black/white or color. The stimulus was presented by using a computer monitor showing a high spatial frequency black/white sinusoidal vertical grating moving horizontally. Alternatively, in three subjects, an isoluminant blue/red color grating was used. The grating moved left or right alternating slowly to prevent afterimages. A small crosshair was provided in the center for fixation. The subjects were instructed to ignore the grating and keep their gaze fixated on the central crosshair.

MRI. To guide anatomical localization, MRI scans were obtained in all subjects. MRI scans were performed on a Magnetom Vision 1.5-T imaging system (Siemens). A magnetization-prepared rapid-gradient echo acquisition was used to acquire anatomic images that consisted of 128 contiguous 1.25-mm-thick sagittal slices. Scanning parameters were repetition time = 10 msec, echo time = 4 msec, inversion time = 300 msec, flip angle = 8°, matrix = 256 × 256 pixels, voxel size = 1 × 1 × 1.25.

PET Image Reconstruction and Registration. Two types of images were created from the dynamic PET scan. First, all 180 sec of data were summed. The resulting images underwent coregistration for correction of head movement between scans by using in-house software (14). Then 40-sec summed images were made from the dynamic data starting ≈6 sec after the [^{15}O]water bolus began entry into the brain as judged by the rise in counts. This 40-sec image was corrected for head motion with the spatial transformation matrix calculated from aligning the 180-sec summed images. Quantitative global CBF values were calculated from the 40-sec data (15) after masking the brain data with a 42% threshold applied to the summed [^{15}O]water image. The 40-sec image of [^{15}O]water was also normalized for whole-brain activity and used to calculate qualitative changes in regional CBF (15).

Volume of Interest (VOI) Analysis. For each subject, an image of visual cortex activation after saline injection was created by averaging the two subtraction images, $CBF_2 - CBF_1$ and $CBF_6 - CBF_5$. An image of visual cortex activation after lactate injection was created from the subtraction image: $CBF_4 - CBF_3$. To create VOIs for analysis, these two subtraction images (saline and lactate) were averaged and smoothed with a 3D Gaussian filter (0.4 cycles per pixel cutoff). Final subtraction image resolution was ≈13 mm full-width half-maximum.

For each subject's final subtraction scan, three differently sized VOIs were created by selecting thresholds that result in visual cortex VOIs of ≈2,000 pixels (equal to 27 cm^3), 1,000 pixels (equal to 12 cm^3), and 300 pixels (equal to 4.1 cm^3). These are abbreviated VOI-2000, VOI-1000, and VOI-300, respectively. All VOIs were confirmed to be centered over the primary visual cortex by comparing location to coregistered MRI images. These VOIs were applied to each of the six normalized 40-sec scans to obtain the qualitative CBF data for each region.

Statistical Analysis. The mean and SD values across subjects (n = 7) of the regional CBF and the global CBF for each of the six states (CBF_1, CBF_2, CBF_3, CBF_4, CBF_5, and CBF_6) were calculated and analyzed by using t tests (two-tailed paired, significance set at $P < 0.05$, and df = 6 for all tests). An estimate

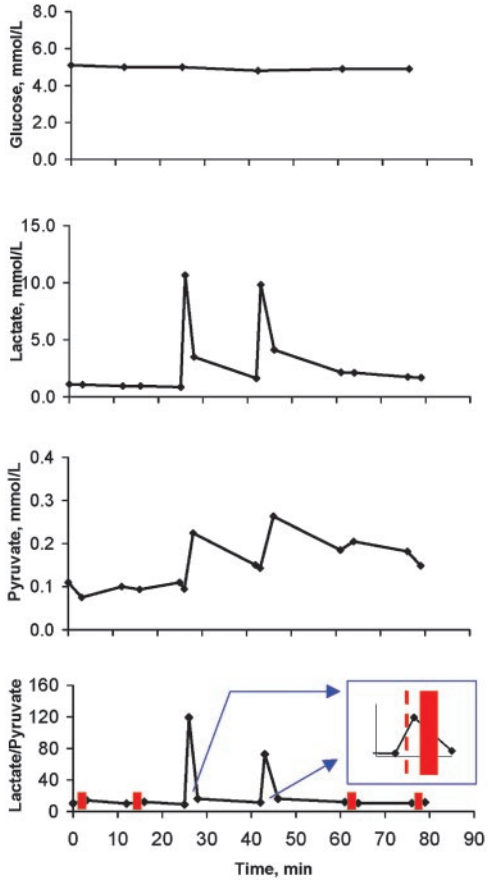

Fig. 1. Blood values for glucose, lactate, pyruvate, and the lactate/pyruvate ratio. *Inset* illustrates the start time of lactate injection (red dashed line) and the PET scan (red bar). The values are means for seven subjects. The values and SDs for all measurements are presented in Table 2.

Table 2. Global CBF and blood glucose, lactate, pyruvate, and lactate/pyruvate ratio at different stages

	Saline		Lactate		Saline	
Parameter	Rest	Activation	Rest	Activation	Rest	Activation
Global CBF, ml/100 g per min	48.8 ± 11.2	47.4 ± 8.3	47.6 ± 14.0	50.5 ± 13.1	49.7 ± 9.9	50.7 ± 10.9
Glucose, mmol/liter	5.1 ± 0.4	5.0 ± 0.2	5.0 ± 0.5	4.8 ± 0.4	4.9 ± 0.4	4.9 ± 0.3
Lactate, mmol/liter						
Before lactate injection			0.8 ± 0.03	1.6 ± 0.03		
Before PET scan	1.1 ± 0.7	0.9 ± 0.5	10.7 ± 2.8*	9.8 ± 2.4*	2.1 ± 0.3*	1.7 ± 0.4*
After PET scan	1.1 ± 0.6	0.9 ± 0.4	3.5 ± 0.2*	4.1 ± 0.2*	2.1 ± 0.3*	1.7 ± 0.4*
Pyruvate, mmol/liter						
Before lactate injection			0.11 ± 0.04	0.15 ± 0.04		
Before PET scan	0.11 ± 0.06	0.10 ± 0.04	0.09 ± 0.02	0.14 ± 0.04	0.19 ± 0.06*	0.18 ± 0.03*
After PET scan	0.08 ± 0.04	0.09 ± 0.05	0.22 ± 0.05*	0.26 ± 0.05*	0.21 ± 0.02*	0.15 ± 0.04*
Lactate/pyruvate ratio						
Before lactate injection			8.9 ± 3.2	11.6 ± 4.2		
Before PET scan	10.3 ± 4.1	10.2 ± 2.9	119.3 ± 46.3*	72.6 ± 23.6*	12.1 ± 2.7	10.5 ± 2.0
After PET scan	14.3 ± 3.2	12.3 ± 7.4	16.2 ± 3.8	16.1 ± 3.4	10.7 ± 1.2	11.6 ± 2.3

Values are means ± SD; $n = 7$. *, Significant change compared to rest baseline before PET scan (two-tailed paired t test; $P < 0.05$).

of mean serum lactate, pyruvate, or lactate/pyruvate ratio during the PET scan was calculated by averaging the prescan and postscan measurements for each substrate. The mean values were used in a two-tailed Pearson analysis of correlation between the percent increase in plasma lactate, pyruvate, and the lactate/pyruvate ratio and the lactate-related increase in percent CBF response to visual stimulation. The percent increase in plasma lactate, pyruvate, and the lactate/pyruvate ratio after lactate injection was calculated from the average of mean values corresponding to CBF_1 and CBF_2 ($L/P_{CBF1–2}$ for the lactate/pyruvate ratio) and the average of the mean values corresponding to the CBF_3 and CBF_4 ($L/P_{CBF3–4}$ for the lactate/pyruvate ratio) as follows (shown for the lactate/pyruvate ratio): $\Delta\%\text{lactate/pyruvate} = 100 \times [(L/P_{CBF\text{-}3}) - (L/P_{CBF1–2})]/(L/P_{CBF1–2})$. The percent increases in CBF during activation with saline or lactate injection were calculated as $\Delta\%CBF_S = 100 \times (CBF_2 - CBF_1)/CBF_1$ and $\Delta\%CBF_L = 100 \times (CBF_4 - CBF_3)/CBF_3$, respectively. The regional CBF values for achromatic and color stimuli were compared by using a two-tailed unpaired t test ($P < 0.05$).

Results

Table 1 gives mean and SD values for arterial blood gas measurements and demographic data for each of the seven subjects. There were no significant changes in these parameters during the study.

Fig. 1 illustrates changes in mean arterial blood lactate, pyruvate, lactate/pyruvate ratio, and glucose throughout the study. There were no blood glucose fluctuations during the study. Lactate levels increased ≈10-fold at the end of each lactate bolus injection, then dropped significantly during the PET scan over the next 3 min. However, lactate levels did not completely return to baseline (first pair of saline PET scans, CBF_1 and CBF_2) and were ≈2-fold higher during the second pair (CBF_5 and CBF_6) of saline PET scans (Table 2 and Fig. 1). Pyruvate levels were almost unchanged at the end of the first lactate injection, but 3 min later they increased ≈2-fold compared with baseline. Similar to lactate levels, pyruvate levels remained 2-fold higher than baseline during CBF_5 and CBF_6 scans (Table 2 and Fig. 1). The plasma lactate/pyruvate ratio increased dramatically (7- to 12-fold) after each lactate injection but returned to baseline over the next 3 min; it did not increase during the CBF_5 and CBF_6 scans (Table 2 and Fig. 1).

Fig. 2 illustrates a parasagittal brain slice in which CBF was substantially increased in the visual cortex in response to visual stimulation. Local CBF in the visual cortex as measured by [^{15}O]water activity increased significantly during visual stimulation in all selected VOIs (Fig. 3): $\Delta\%CBF_S$ values were 17% (VOI-2000), 19% (VOI-1000), and 22% (VOI-300). Compared with saline injection, visual stimulation after lactate injection resulted in significantly larger CBF increases with $\Delta\%CBF_L$ values of 23% (VOI-2000: $t = 3.09$, $P = 0.022$, two-tailed paired t test), 26% (VOI-1000: $t = 2.63$, $P = 0.039$, two-tailed paired t test), and 31% (VOI-300: $t = 2.63$, $P = 0.039$, two-tailed paired t test). The percent increase in $\Delta\%CBF$, i.e., the percent lactate augmentation of CBF response, was calculated as 100 ×

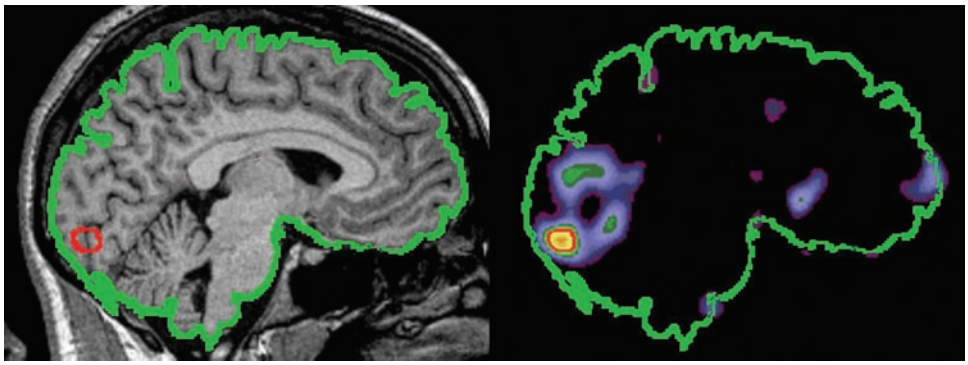

Fig. 2. Coregistered sagittal MRI (left) and PET (right) images from a single subject. PET image is a subtraction of a normalized [^{15}O]water lactate resting scan from a lactate activation scan. The area delineated with a red line is a representative of the largest selected region, VOI-2000.

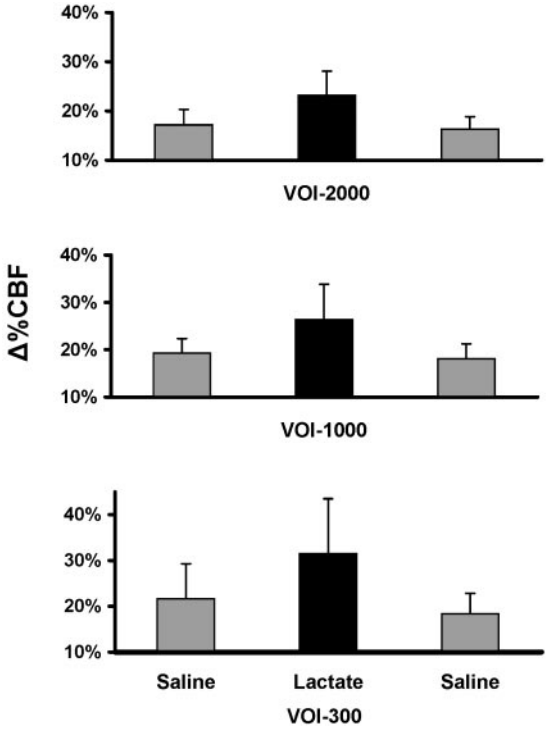

Fig. 3. The percent increase in CBF (Δ%CBF) caused by visual stimulation with and without bolus lactate injection for all three sizes of VOIs examined.

($\Delta\%CBF_L - \Delta\%CBF_S$)/$\Delta\%CBF_S$; thus, the bolus injection of lactate augmented the percent CBF response to the visual stimulation by 38% (VOI-2000), 38% (VOI-1000), and 53% (VOI-300). In the resting state, there was no significant difference in qualitative visual cortex CBF between lactate and saline scans (VOI-2000: two-tailed paired t test, $t = 1.08$, $P = 0.32$; VOI-1000: $t = 1.36$, $P = 0.22$, two-tailed paired t test; and VOI-300: $t = 1.67$, $P = 0.15$, two-tailed paired t test). In the second saline pair of studies, CBF response to visual activation was similar to that in the first saline pair of studies in all VOIs (Fig. 3). Global CBF values were stable throughout the study (Table 2).

Lactate-augmented CBF increases ($\Delta\%CBF_L - \Delta\%CBF_S$) correlated to the elevations in plasma lactate/pyruvate ratios in VOI-2000 and VOI-1000 but was not significant in VOI-300 (Pearson correlation; $r = 0.913$ and $P = 0.004$ for VOI-2000, $r = 0.947$ and $P = 0.01$ for VOI-1000, and $r = 0.598$ and $P = 0.156$ for VOI-300). The augmentation in CBF response also correlated to changes in plasma lactate levels, but this correlation was significant only for VOI-1000 (Pearson correlation; $r = 0.748$ and $P = 0.053$ for VOI-2000, $r = 0.776$ and $P = 0.040$ for VOI-1000, and $r = 0.605$ and $P = 0.15$ for VOI-300). There was no significant correlation between lactate-augmented CBF changes and changes in plasma pyruvate levels (Pearson correlation; $r = 0.216$ and $P = 0.643$ for VOI-2000, $r = 0.186$ and $P = 0.69$ for VOI-1000, and $r = 0.209$ and $P = 0.653$ for VOI-300). Fig. 4 shows the correlations for VOI-1000.

We did not find significant difference in Δ%CBF between the subjects with color visual stimulus ($n = 3$) and those stimulated with achromatic grating ($n = 4$). CBF response to visual stimulation has a nonsignificant tendency to be higher with achromatic stimulus for both saline and lactate measures. For VOI-1000, CBF response was 21% ($\Delta\%CBF_S$) and 27% ($\Delta\%CBF_L$) for achromatic grating and 17% and 25% for color stimulus, respectively (two-tailed unpaired t test; $t = 1.58$, df = 5, and $P = 0.17$ for baseline and $t = 0.43$, df = 5, and $P = 0.69$ for lactate injection). The percent lactate augmentation of CBF response with a color stimulus was nonsignificantly higher compared with an achromatic stimulus. For VOI-1000, CBF response was 32% (increase from lactate by using achromatic stimulus) and 46% (increase from lactate by using color stimulus), respectively (two-tailed unpaired t test, $t = 0.45$, df = 5, $P = 0.67$).

Discussion

Our data demonstrate that lactate injection augments the increase in CBF evoked by visual stimulation without affecting resting visual cortex CBF or whole-brain CBF. This lactate-augmented CBF increase was substantial in all three differently sized VOIs. The augmented CBF correlated strongly with the plasma lactate/pyruvate ratio, less strongly with plasma lactate, and not at all with plasma pyruvate.

Our findings suggest a link between CBF regulation and the redox state of the cell (the $NADH/NAD^+$ or lactate/pyruvate ratio) and help to characterize the mechanisms of CBF increase associated with physiological brain activation (Fig. 5). The fact that lactate injection did not alter CBF in the resting brain but significantly augmented CBF increase in activated brain is of primary importance, because it shows that lactate does not appear to modulate CBF directly. Furthermore, the data support the hypothesis that it is the increase in the lactate/pyruvate ($NADH/NAD^+$) ratio evoked by lactate injection (rather than the molar increase in plasma lactate level *per se*) that augments CBF in activated cortex. In the second saline pair (CBF_5 and CBF_6), lactate levels were ≈2-fold higher (Table 2 and Fig. 1), lactate/pyruvate ratios were at baseline, and no augmentation of the CBF response to activation was seen. This dependence on the lactate/pyruvate ratio rather than lactate alone was also seen in rats in the study that showed that coinjection of lactate and pyruvate had no effect on CBF in stimulated or resting somatosensory cortex, despite the significant increase in plasma lactate

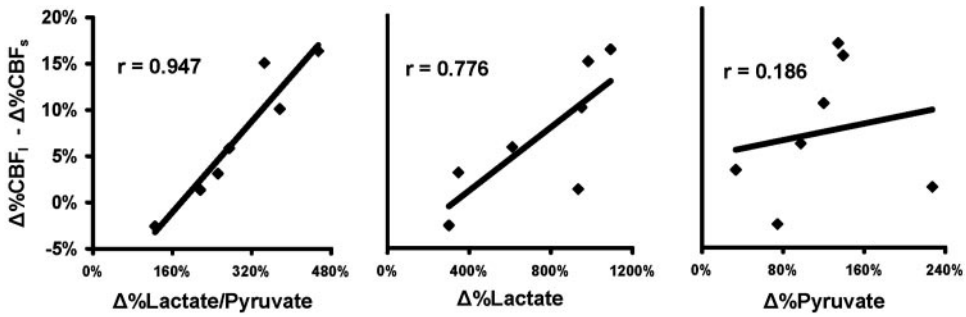

Fig. 4. Correlation between lactate-augmented CBF increases and percent changes in plasma lactate, pyruvate, and the lactate/pyruvate ratio. All CBF values are derived from VOI-1000.

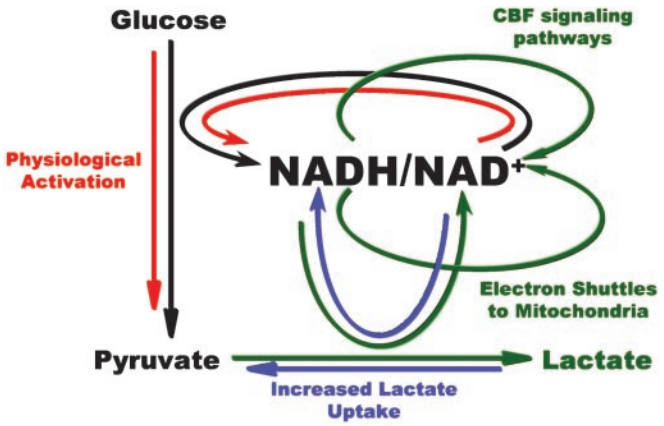

Fig. 5. Mechanisms of increased cytosolic NADH production and regeneration of NAD^+. Black lines indicate known pathways for metabolism and redox regulation in resting brain cells. Red lines indicate the changes associated with physiological activation (e.g., in response to visual stimulation). Green lines highlight main NAD^+-regenerating pathways. Blue lines highlight changes provoked by the injection of lactate.

and pyruvate levels with no elevation of the lactate/pyruvate ratio (8). Finally, our data show the strongest correlation between the magnitude of the CBF augmentation and changes in the lactate/pyruvate ratio.

Because a rise in the lactate/pyruvate ratio is linked to a rise of the $NADH/NAD^+$ ratio, we suggest that the $NADH/NAD^+$ ratio serves as a key cytosolic sensor and, when elevated, can augment the local CBF increases seen in activation. The rationale for this argument is based on several aspects of brain energy metabolism and associated biochemistry.

Generation of metabolic energy from glucose starts with glycolysis, which is a sequence of reactions that converts glucose into pyruvate with concomitant production of ATP (substrate phosphorylation). In normal resting brain cells, pyruvate then enters mitochondria, where it is converted to acetyl-CoA and is completely oxidized to carbon dioxide through the citric acid (Krebs) cycle. Most of glucose-derived ATP is generated in mitochondria as the result of the transfer of electrons from $FADH_2$ and NADH, formed in the citric acid cycle, to oxygen (oxidative phosphorylation).

Before ATP and pyruvate are generated in the cytosol, a hydrogen ion and two electrons must be transferred from glyceraldehyde 3-phosphate (oxidizing it to 1,3-diphosphoglycerate) to free NAD^+ (reducing it to NADH) in a reaction catalyzed by glyceraldehyde-3-phosphate dehydrogenase. To sustain the continued operation of glycolysis, the regeneration of NAD^+ is absolutely necessary, because, otherwise, glycolysis could not proceed beyond glyceraldehyde 3-phosphate and no ATP would be generated by substrate or oxidative phosphorylation (10).

There are several ways to regenerate cytosolic NAD^+. One of the primary ways is a transfer of electrons from NADH to mitochondria by glycerol–phosphate or malate–aspartate shuttles. In the malate–aspartate shuttle, which has been shown to be operative in brain (16–18), electrons are transferred from NADH in the cytosol to oxaloacetate, forming malate, which traverses the inner mitochondrial membrane and is then reoxidized by NAD^+ in the matrix to form NADH. The resulting oxaloacetate does not readily cross the inner mitochondrial membrane, so a transamination reaction is needed to form aspartate, which can be transported to the cytosolic side (10). These shuttles not only allow reoxidation of cytosolic NAD^+ but also provide more ATP (1.5 mol by means of the glycerol–phosphate shuttle or 2.5 mol by means of the malate–aspartate shuttle) by oxidative phosphorylation (10). Blockade of the malate–aspartate shuttle by specific inhibitors is associated with an increase in the cytosolic NADH/NAD ratio (19, 20). Reduction of pyruvate to lactate is another important way to regenerate NAD^+, because it is extremely rapid and coupled to an equimolar reoxidation of NADH generated by glyceraldehyde 3-phosphate to NAD^+ generated by lactate dehydrogenase.

During physiological brain activation, there is good evidence that glycolysis is elevated to a substantially greater degree than oxygen utilization (2, 3, 21), and there is a need for regeneration of greater amounts of NAD^+, requiring an increase in both above-mentioned NAD^+-regenerating mechanisms. Reduction of pyruvate to lactate results in a rise in tissue lactate levels, which has been demonstrated in animals (22, 23) and in humans with magnetic resonance spectroscopy (24–27) during brain activation. It has been proposed that a third pathway for regeneration of NAD^+ occurs during activation, which increases NADH oxidation through signaling pathways that promote production of nitric oxide with subsequent increase in blood flow (8, 11).

Given these NAD^+-regenerating pathways, administration of lactate during activation can be predicted to have specific consequences. Increased tissue lactate (from plasma) will raise the lactate/pyruvate ratio and thereby stop or reverse the cytosolic pyruvate–lactate conversion. This reversal will add significantly to the NADH accumulating by means of glycolysis. The subsequent rise in the $NADH/NAD^+$ ratio should recruit signaling pathways and further increase CBF (Fig. 5), resulting in the effect shown by our data (Fig. 3).

There are several possibilities that explain why lactate injection would be less likely to have an impact on CBF in resting versus activated brain. First, it is important to consider how infused lactate can gain entry into the brain. Early work in anesthetized animals showed that lactate crosses the blood–brain barrier by facilitated diffusion in a stereospecific and saturable manner, and the rate of lactate uptake is much lower than that of glucose (28). However, more recent studies in awake animals and humans demonstrated that the average brain uptake of lactate in resting brain is approximately seven times higher than previously calculated (28), reaching $\approx$50% of that of glucose (29, 30). Although entry of lactate from plasma into resting brain is more rapid than previously thought (31), Lear and Kasliwal (32) have shown that the local transport of lactate is further increased during brain activation, which could lead to an increased effect of the injected lactate.

A second reason for the observed effects of lactate can be inferred from the observation that glucose utilization in resting brain is decreased by addition of lactate. This effect has been demonstrated in incubated rat brain slices (33, 34) and brain cell cultures (35, 36) and *in vivo* by using i.v. (37, 38) or i.p. (31, 39) lactate administration. Under these experimental conditions it is likely that exogenous lactate is oxidized to pyruvate (coupled to the reduction of cytosolic NAD^+ to NADH) and used in mitochondria instead of or in addition to pyruvate produced by glycolysis. Thus, in the resting brain, the cytosolic NADH formed by oxidation of lactate to pyruvate may be balanced by reduced formation of NADH through a reduction in glycolysis. In this scenario, there is limited, if any, excess production of NADH, and the malate–aspartate shuttle could reoxidize cytosolic NADH to NAD^+ without activation of CBF-increasing signaling pathways. We speculate that in activated cortex the increased rate of glycolysis (mediated by activation of phosphofructokinase) (10) will be much less sensitive to inhibition by injected lactate. Thus, in activated cortex, the increased glycolysis and the increased lactate will have an additive effect on NADH production and increase in the $NADH/NAD^+$ ratio.

Our main observations are in agreement with the effects of lactate injection on blood flow in activated whisker barrel cortex,

retina, and visual cortex in rats (8, 11). To our knowledge, there are no prior reports in the literature concerning the effects of lactate on activated CBF in humans.

Some studies have reported on the effect of lactate on resting CBF. Stewart *et al.* (40) assessed hemispheric CBF by using single-photon-emission computed tomography with ^{133}Xe inhalation in patients with panic disorders and in normal control subjects. They reported a marked CBF increase in both control subjects and patients who did not panic. Patients who did show lactate-induced panic experienced either a minimal increase or a decrease in hemispheric CBF. None of the subjects in our study experienced any symptoms of a panic attack. In similar clinical groups, Reiman *et al.* (41) studied regional CBF by using PET and found no changes in regional CBF during lactate infusion in either normal controls or nonpanicking patients, whereas, during panic attacks, CBF was significantly increased bilaterally in several brain areas. Interpretation of these results and comparison with observations in our study is difficult, because, in their studies (40, 41), the CBF measurements during lactate infusion were obtained in the resting state only; lactate was continuously infused for 20–30 min rather than given as bolus; total dose of lactate injected was 4- to 5-fold higher than in our study; and no measurements of plasma lactate, pyruvate, and the lactate/pyruvate ratios were reported. It is of interest that, among other theories, changes in the redox state (lactate/pyruvate ratio) in the brain cells were suggested to be involved in the development of panic attacks (42).

We did not find a significant difference in CBF responses between color and achromatic stimuli. The percent of CBF increase caused by visual stimulation with or without lactate was nonsignificantly higher with achromatic grating, which could be explained by the more powerful action of the higher spatial frequency achromatic stimulus. As designed, both stimuli resulted in CBF activation of a magnitude much less than the maximal values (≈50%) reported in the literature (2, 3). In general, submaximal stimulation is probably preferable for studies in which the aim is to investigate the augmentation of CBF; near-maximal CBF responses could preclude observing further increases in CBF, e.g., induced by lactate or other CBF-modifying agents.

In conclusion, we found that lactate injection significantly augmented the CBF response to physiological stimulation of the visual cortex but had no significant effect on the resting CBF or the whole-brain CBF. These lactate-induced CBF increases correlated with elevations in plasma lactate/pyruvate ratios and plasma lactate levels but not in plasma pyruvate levels. Our data support the hypothesis that the $NADH/NAD^+$ ratio modulates CBF regulatory mechanisms. The $NADH/NAD^+$ ratio, being a sensor of the need for regeneration of cytosolic NAD^+ (one of the most vital aspects of brain cell functioning), when substantially elevated, activates signaling pathways to increase the local CBF. Further work with other modifiers of NADH would be useful to confirm and expand this hypothesis regarding the relationship between the cytosolic $NADH/NAD^+$ ratio and CBF during physiological activation.

We thank Joseph R. Williamson for comments and advice and Lenis Lich for skilled technical assistance in PET imaging. This work was supported by National Institutes of Health/National Institute of Neurological Disorders and Stroke Grant P50 NS-06833 and National Institutes of Health/National Heart, Lung, and Blood Institute Grant P01 NL-13851.

1. Siesjo, B. K. (1978) *Brain Energy Metabolism* (Wiley, New York).
2. Fox, P. T. & Raichle, M. E. (1986) *Proc. Natl. Acad. Sci. USA* **83,** 1140–1144.
3. Fox, P. T., Raichle, M. E., Mintun, M. A. & Dence, C. (1988) *Science* **241,** 462–464.
4. Kim, S. G. & Ugurbil, K. (1997) *Magn. Reson. Med.* **38,** 59–65.
5. Blomqvist, G., Seitz, R. J., Sjogren, I., Halldin, C., Stone-Elander, S., Widen, L., Solin, O. & Haaparanta, M. (1994) *Acta Physiol. Scand.* **151,** 29–43.
6. Powers, W. J., Hirsch, I. B. & Cryer, P. E. (1996) *Am. J. Physiol.* **270,** H554–H559.
7. Mintun, M. A., Lundstrom, B. N., Snyder, A. Z., Vlassenko, A. G., Shulman, G. L. & Raichle, M. E. (2001) *Proc. Natl. Acad. Sci. USA* **98,** 6859–6864.
8. Ido, Y., Chang, K., Woolsey, T. A. & Williamson, J. R. (2001) *FASEB J.* **15,** 1419–1421.
9. Williamson, D. H., Lund, P. & Krebs, H. A. (1967) *Biochem. J.* **103,** 514–527.
10. Stryer, L. (1995) *Biochemistry* (Freeman, New York).
11. Ido, Y., Chang, K. & Williamson, J. R. (2004) *Proc. Natl. Acad. Sci. USA* **101,** 653–658.
12. Oldfield, R. C. (1971) *Neuropsychologia* **9,** 97–113.
13. Wienhard, K., Dahlbom, M., Eriksson, L., Michel, C., Bruckbauer, T., Pietrzyk, U. & Heiss, W. D. (1994) *J. Comput. Assist. Tomogr.* **18,** 110–118.
14. Snyder, A. Z. (1996) in *Quantification of Brain Function Using PET*, eds. Myer, R., Cunningham, V. J., Bailey, D. L. & Jones, T. (Academic, San Diego), pp. 131–137.
15. Fox, P. T. & Mintun, M. A. (1989) *J. Nucl. Med.* **30,** 141–149.
16. Brand, M. D. & Chappell, J. B. (1974) *Biochem. J.* **140,** 205–210.
17. Minn, A. & Gayet, J. (1977) *J. Neurochem.* **29,** 873–881.
18. Dennis, S. C. & Clark, J. B. (1978) *Biochem. J.* **172,** 155–162.
19. Kauppinen, R. A., Sihra, T. S. & Nicholls, D. G. (1987) *Biochim. Biophys. Acta* **930,** 173–178.
20. Cheeseman, A. J. & Clark, J. B. (1988) *J. Neurochem.* **50,** 1559–1565.
21. Mintun, M. A., Vlassenko, A. G., Shulman, G. L. & Snyder, A. Z. (2002) *NeuroImage* **16,** 531–537.
22. Ueki, M., Linn, F. & Hossmann, K. A. (1988) *J. Cereb. Blood Flow Metab.* **8,** 486–494.
23. Madsen, P. L., Cruz, N. F., Sokoloff, L. & Dienel, G. A. (1999) *J. Cereb. Blood Flow Metab.* **19,** 393–400.
24. Prichard, J., Rothman, D., Novotny, E., Petroff, O., Kuwabara, T., Avison, M., Howseman, A., Hanstock, C. & Shulman, R. (1991) *Proc. Natl. Acad. Sci. USA* **88,** 5829–5831.
25. Sappey-Marinier, D., Calabrese, G., Fein, G., Hugg, J. W., Biggins, C. & Weiner, M. W. (1992) *J. Cereb. Blood Flow Metab.* **12,** 584–592.
26. Frahm, J., Kruger, G., Merboldt, K. D. & Kleinschmidt, A. (1996) *Magn. Reson. Med.* **35,** 143–148.
27. Urrila, A. S., Hakkarainen, A., Heikkinen, S., Vuori, K., Stenberg, D., Hakkinen, A. M., Lundbom, N. & Porkka-Heiskanen, T. (2003) *J. Cereb. Blood Flow Metab.* **23,** 942–948.
28. Pardridge, W. M. & Oldendorf, W. H. (1977) *J. Neurochem.* **28,** 5–12.
29. Hassel, B. & Brathe, A. (2000) *J. Cereb. Blood Flow Metab.* **20,** 327–336.
30. Knudsen, G. M., Paulson, O. B. & Hertz, M. M. (1991) *J. Cereb. Blood Flow Metab.* **11,** 581–586.
31. Thurston, J. H., Hauhart, R. E. & Schiro, J. A. (1983) *J. Cereb. Blood Flow Metab.* **3,** 498–506.
32. Lear, J. L. & Kasliwal, R. K. (1991) *J. Cereb. Blood Flow Metab.* **11,** 576–580.
33. Ide, T., Steinke, J. & Cahill, G. F., Jr. (1969) *Am. J. Physiol.* **217,** 784–792.
34. Fernandez, E. & Medina, J. M. (1986) *Biochem. J.* **234,** 489–492.
35. Tabernero, A., Vicario, C. & Medina, J. M. (1996) *Neurosci. Res.* **26,** 369–376.
36. Bliss, T. M. & Sapolsky, R. M. (2001) *Brain Res.* **899,** 134–141.
37. Harding, J. E. & Charlton, V. E. (1990) *J. Dev. Physiol.* **14,** 139–146.
38. Smith, D., Pernet, A., Hallett, W. A., Bingham, E., Marsden, P. K. & Amiel, S. A. (2003) *J. Cereb. Blood Flow Metab.* **23,** 658–664.
39. Miller, A. L., Kiney, C. A. & Staton, D. M. (1984) *Brain Res.* **316,** 33–40.
40. Stewart, R. S., Devous, M. D., Sr., Rush, A. J., Lane, L. & Bonte, F. J. (1988) *Am. J. Psychiatry* **145,** 442–449.
41. Reiman, E. M., Raichle, M. E., Robins, E., Mintun, M. A., Fusselman, M. J., Fox, P. T., Price, J. L. & Hackman, K. A. (1989) *Arch. Gen. Psychiatry* **46,** 493–500.
42. Carr, D. B. & Sheehan, D. V. (1984) *J. Clin. Psychiatry* **45,** 323–330.